Available online at www.sciencedirect.com
ScienceDirect
Ceramics International 37 (2011) 1033–1037
CERAMICS INTERNATIONAL
www.elsevier.com/locate/ceramint

Structure and dielectric characteristics of $Ca(Fe_{1/2}Ta_{1/2})O_3$ complex perovskite ceramics

Xin Lv, Zhuo Wang, Xiang Ming Chen *

Laboratory of Dielectric Materials, Department of Materials Science and Engineering, Zhejiang University, Hangzhou 310027, China

Received 30 September 2010; received in revised form 17 October 2010; accepted 12 November 2010
Available online 25 December 2010

Abstract

$Ca(Fe_{1/2}Ta_{1/2})O_3$ complex perovskite ceramics have been prepared and characterized in the crystal structure and microstructures, and the dielectric characteristics have been evaluated over a broad temperature and frequency range. There are two dielectric relaxations in low and high temperature ranges, respectively. Differing from the situation for $Ba(Fe_{1/2}Ta_{1/2})O_3$, $Sr(Fe_{1/2}Ta_{1/2})O_3$ and $Ba(Fe_{1/2}Nb_{1/2})O_3$, O_2-annealing has little effect on the dielectric properties of $Ca(Fe_{1/2}Ta_{1/2})O_3$, and the much lower dielectric constant and low loss are ascribed to the low concentration of Fe^{2+} according to the XPS measurements. The microwave dielectric properties (at 5.38 GHz) for $Ca(Fe_{1/2}Ta_{1/2})O_3$ ceramics are obtained as: $\varepsilon_r = 30.7$, $Qf = 3070$ GHz.

Key words : B. X-ray methods; C. Dielectrics properties; D. Perovskites

1. Introduction

The complex perovskites have been intensively investigated over the past 20 years. These kinds of materials possess excellent properties with intriguing physical phenomena. In lead-based complex perovskites, the relaxor ferroelectric properties [1] and piezoelectric response [2] make $Pb(Mg_{1/3}Nb_{2/3})O_3$ and $Pb(Zr,Ti)O_3$ suitable for practical applications. The relaxor ferroelectric behaviors in $Pb(Mg_{1/3}Nb_{2/3})O_3$ ceramics [3] have attracted increasing scientific interests in understanding the physical nature of such unique dielectric characteristics in lead-based complex perovskites [4].

On the other hand, in lead-free system, most of the Ba-, Sr-, and Ca-based complex perovskites, such as $Ba(Mg_{1/3}Ta_{2/3})O_3$, $Ba(Zn_{1/3}Ta_{2/3})O_3$ and $Ca(Zn_{1/3}Ta_{2/3})O_3$, are generally known as low-loss microwave dielectric materials [5–7]. Recently, some Fe-containing perovskites with B-site 1:1 disordered structure were extensively investigated due to the giant dielectric response. These materials generally exhibit a giant dielectric constant step followed by a sharp drop in dielectric constant without any detectable phase transition [8–10]. The giant dielectric response has been observed in $Ba(Fe_{1/2}Ta_{1/2})O_3$, $Sr(Fe_{1/2}Ta_{1/2})O_3$ and $Ba(Fe_{1/2}Nb_{1/2})O_3$ ceramics, and similar dielectric relaxation behavior but much lower dielectric constant step is observed in $Ca(Fe_{1/2}Nb_{1/2})O_3$ ceramics [11]. There are two dielectric abnormities in these materials, usually one of the abnormal dielectric constant peaks at higher temperature will disappear after annealing in the oxygen.

In the present work, $Ca(Fe_{1/2}Ta_{1/2})O_3$ ceramics are prepared and characterized. The crystal structure and microstructures are determined, and the dielectric characteristics are evaluated over a wide temperature and frequency range. The mixed-valent structure is investigated by XPS measurements.

2. Experimental

$Ca(Fe_{1/2}Ta_{1/2})O_3$ ceramics were prepared by a standard solid-state reaction process from reagent powders of $CaCO_3$ (99.99%), Fe_2O_3 (>99%) and Ta_2O_5 (99.99%) as the raw materials. The raw materials were mixed by ball milling with zirconia media in ethanol for 24 h, and then the mixtures were heated at 1473 K in air for 3 h after drying to yield $Ca(Fe_{1/2}Ta_{1/2})O_3$. The calcined powders with 5% of polyvinyl alcohol (PVA) were pressed into the disks measuring 10 mm in diameter and 2 mm in height under a pressure about 98 MPa, and then sintered at 1523 K in air for 3 h. After cooling from the

* Corresponding author.
E-mail address: Xmchen59@zju.edu.cn (X.M. Chen).

0272-8842/$36.00
doi:10.1016/j.ceramint.2010.11.036

sintering temperature to 1373 K at a rate of 2 K/min, the ceramics were cooled with furnace. The bulk density of specimens was higher than 98% of theoretical density.

The crystal structure of sintered samples after crushing was determined by powder X-ray diffraction (XRD) analysis, using Cu $K\alpha$ radiation (Dmax 3B, Rigaku, Tokyo, Japan). The Rietveld refinement for the XRD data was performed using the FULLPOF program [12]. The microstructures were observed by scanning electron microscopy, SEM (S-1800, Hitachi, Tokyo, Japan), and X-ray photoemission spectroscopy (XPS) experiments were carried out to evaluate the mixed-valent structure on a PHI-5000C ESCA system (Perkin Elmer, MA) with Mg $K\alpha$ radiation ($h\nu = 1253.6$ eV) or Al $K\alpha$ radiation ($h\nu = 1486.6$ eV). The experimental curve was fitted with a program (XPS-PEAK4.1) that made use of a combination of Gaussian–Lorentzian lines.

The dielectric characteristics of the present ceramics were measured with a broadband dielectric spectrometer (Turnkey concept 50, Novocontrol Technologies, Germany) in a broader range of temperature (133–573 K) and frequency (10–10,00,000 Hz), and the silver paste was adopted as the electrode. The microwave dielectric constant ε_r and quality factor Q were evaluated by Hakki–Coleman method and cavity method using vector network analysis (Agilent 8753ES, Agilent Technologies Inc., Palo Alto, CA), respectively [13]. Because Q factor generally varies inversely with the frequency in the microwave region, the product of Qf was used to evaluate the dielectric loss instead of Q. In order to understand the origins of the dielectric characteristics, some samples were annealed at 1273 K for 6 h in oxygen.

3. Results and discussion

Microstructures of the as-sintered surfaces of $Ca(Fe_{1/2}Ta_{1/2})O_3$ ceramics are shown in Fig. 1. Dense ceramics with homogenous microstructure are obtained. The grain size of the ceramics is about 1.8 μm.

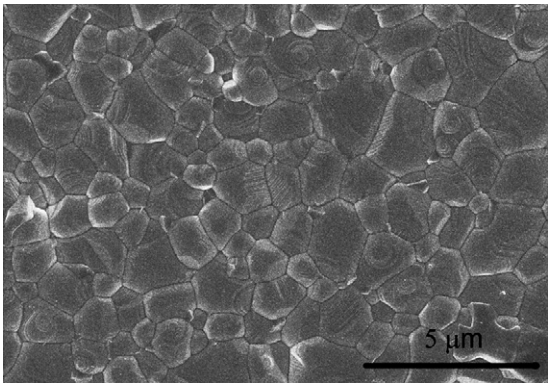

Fig. 1. SEM micrograph of $Ca(Fe_{1/2}Ta_{1/2})O_3$ dense ceramics.

Fig. 2 shows the results of Rietveld analysis for the XRD profiles of $Ca(Fe_{1/2}Ta_{1/2})O_3$ ceramics, where a single-phase with orthorhombic crystal structure in space group *Pbnm* (62) is determined. The lack of reflection at $2\theta = 18.8^\circ$ in the XRD pattern indicates that the B-site cations are disordering [14]. According to XRD results, the cations ordering is similar to the B-site cation ordering of $Ca(Fe_{1/2}Nb_{1/2})O_3$ [11]. But as the increasing of the B-site cations diameter ratio the ordering degree increases. The experimental parameters of XRD and the refined structural parameters are given in Table 1 Moreover, the selected bond lengths and angles are summarized in Table 2 The tolerance factor (t) of the ceramics is 0.947, which is less than 0.965. According to Reaney's report [15], the tilting of oxygen octahedra occurs in both anti-phase and in-phase. The superlattice reflections (marked in bold) which indicate that oxygen octahedrals around Fe^{3+}/Ta^{5+} in $Ca(Fe_{1/2}Ta_{1/2})O_3$ are detected in the XRD patterns. According to Glazer's theory [16], the anti-phase tilting along pseudocubic [1 0 0] direction

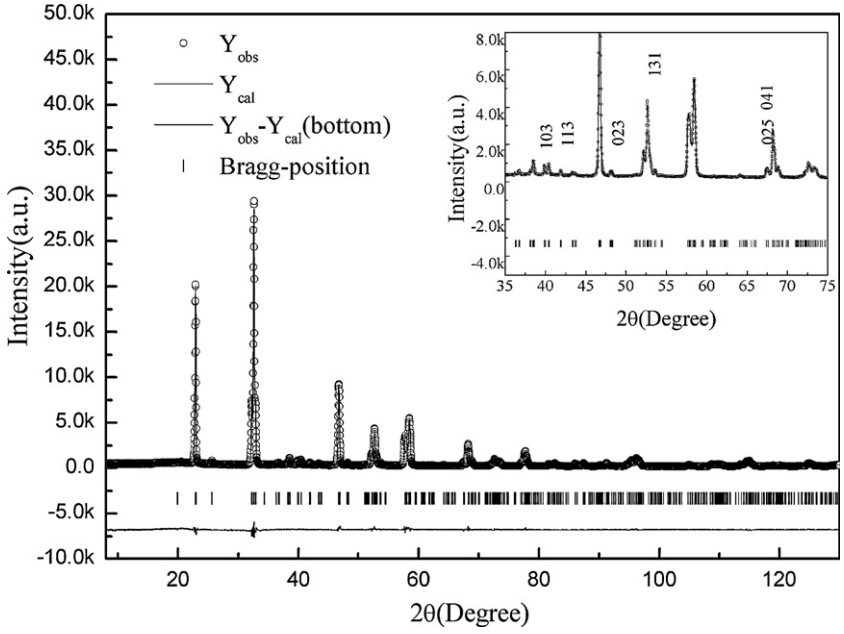

Fig. 2. Profile fits for the rietveld refinement of $Ca(Fe_{1/2}Ta_{1/2})O_3$ dense ceramics. The inset is the enlargement of profile fits at low 2θ ranges.

Table 1
Refined Structure Parameters of $Ca(Fe_{1/2}Ta_{1/2})O_3$.[a]

Atom	Site	x	y	z	B_{iso} (Å^2)	Occupancy
Ca	4*c*	−0.0140 (84)	0.45782 (39)	0.25000	1.344 (51)	0.500
Ta	4*a*	0.00000	0.00000	0.00000	0.655 (19)	0.250
Fe	4*a*	0.00000	0.00000	0.00000	0.655 (19)	0.250
O1	8*d*	0.70806 (100)	0.21152 (98)	0.05204 (72)	0.356 (88)	1.000
O2	4*c*	0.07534 (120)	0.02940 (137)	0.25000	0.356 (88)	0.500

[a]Lattice parameters: $a = 5.4513$ (2) Å, $b = 5.5499$ (2) Å, $c = 7.76268$ (3) Å, $V = 234.856$ (0) Å^3, space group *Pbnm* (62). Agreement indices: R_{wp} (%) = 7.82, R_p (%) = 5.62, $\chi^2 = 3.30$.

Table 2
Selected bond distance for $Ca(Fe_{1/2}Ta_{1/2})O_3$.

Bond distances (Å)		Bond angles (°)	
Ca–O(1)	2.555 (6) × 2	O(1)–Fe/Ta–O(1)	88.7 (4) × 2
	2.801 (6) × 2		91.3 (4) × 2
	2.338 (6) × 2		180.0 (5) × 2
	3.413 (6) × 2	O(1)–Fe/Ta–O(2)	85.4 (4) × 2
Ca–O(2)	2.427 (8)		89.2 (4) × 2
	2.424 (8)		90.8 (3) × 2
	3.086 (8)		94.6 (3) × 2
	3.209 (8) × 2	O(2)–Fe/Ta–O(2)	180.0 (14)
Fe/Ta–O(1)	2.003 (6) × 2		
	2.018 (5) × 2		
Fe/Ta–O(2)	1.9903 (15) × 2		

(a^-) of the oxygen octahedra is related to the reflections of odd–odd–odd with $k \neq l$ and the in-phase tilting along pseudocubic [0 1 0] direction (b^+) is related to the odd–even–odd reflections with $h \neq l$. So the (1 3 1), (1 1 3) reflections indicate a^- tilting and the (1 0 3) reflection indicates ab^+ tilting. Therefore, according to Glazer's notation [17], the tilting mechanism is consistent with the orthorhombic $a^-a^-b^+$ tilt system. The remaining bolded in the XRD patterns reflections (2 0 3), (0 4 1), (2 0 5), which $N = 13$, 17 and 29 not being consistent with the tilting mechanisms. As a result, it is suggested that these reflections arise from antiparallel cation displacement [17]. These reflections are related with the Ca atoms displace exactly along the $\langle 1\bar{1}0 \rangle$ pseudocubic directions. Fig. 3 gives the crystal structure of the $Ca(Fe_{1/2}Ta_{1/2})O_3$. The arrows indicated the direction of Ca displacements (at height 1/4*c*).

The dielectric constant (ε') and dielectric loss (tan δ) for the as-sintered $Ca(Fe_{1/2}Ta_{1/2})O_3$ ceramics are shown as functions of frequency and temperature in Fig. 4. A dielectric abnormity with strong frequency dispersion is observed in the present ceramics in the temperatures ranged 153–382 K, and the critical temperature for the dielectric abnormity increases with increasing frequency. The ε' (T) peak corresponding to the low temperature dielectric abnormity is not so obvious and only a quite small step can be detected in the magnitude of dielectric constant. Meanwhile, the tan δ (T) shows strong frequency dispersion and moves toward higher temperature with increasing frequency. While the considerable increase in both ε' (T) and tan δ (T) at the temperature above 400 K is observed for the as-sintered $Ca(Fe_{1/2}Ta_{1/2})O_3$ ceramics at low frequencies, and this differs from that observed in $R(Fe_{1/2}M_{1/2})O_3$ (R = Ba, Sr; M = Ta, Nb) ceramics [8–11], where a high temperature dielectric relaxation is also observed.

The low temperature dielectric relaxation can be modeled with the Arrhenius law as shown in Fig. 5:

$$f = f_0 \exp\left(\frac{-E_a}{kT}\right) \quad (1)$$

where f_0 is the pre-exponential term, E_a is the activation energy, and k is the Boltzmann constant. The best fit to Eq. (1) yields

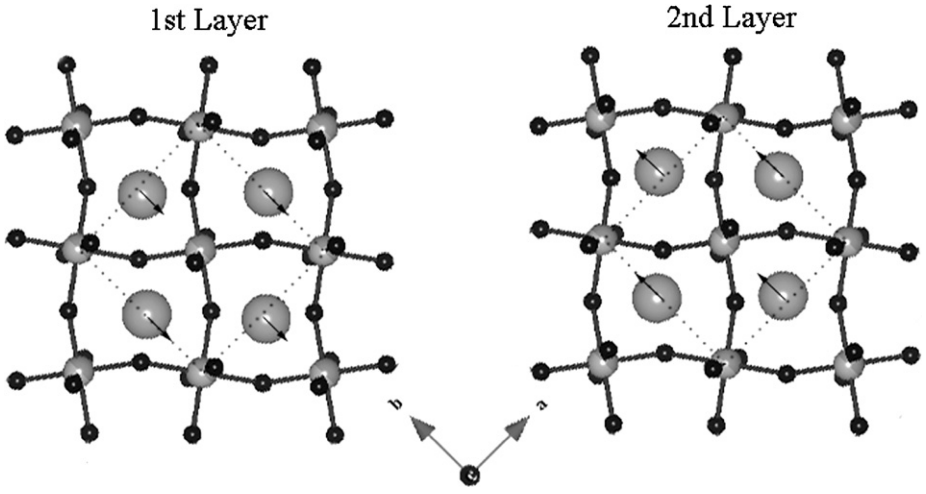

Fig. 3. Crystal structure of $Ca(Fe_{1/2}Ta_{1/2})O_3$ ceramic drawn with VENUS [19].

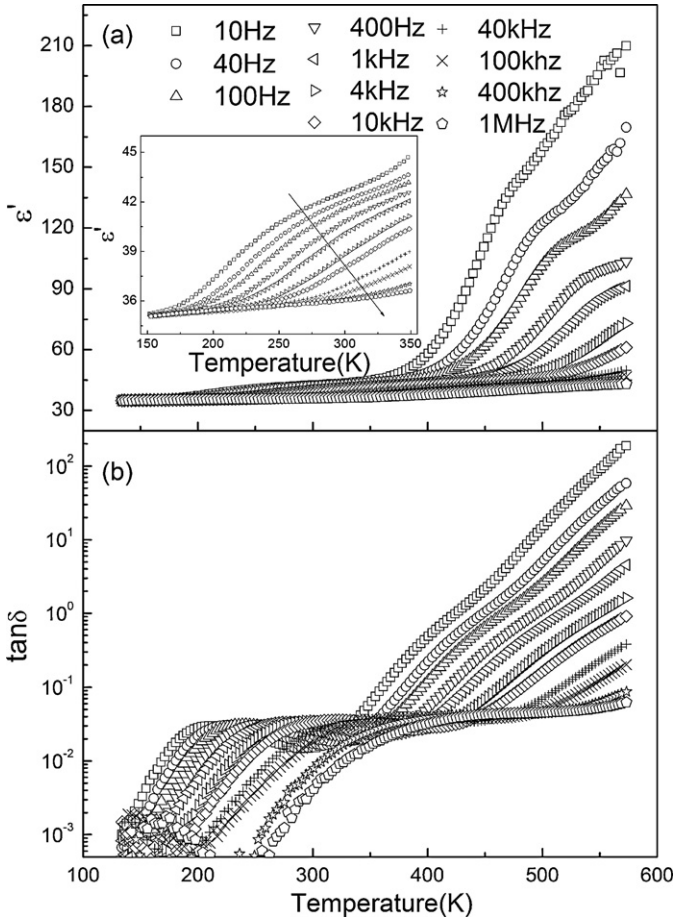

Fig. 4. Temperature dependence of (a) dielectric constant, the inset is the enlargement of dielectric constant at low temperature ranges and (b) dielectric loss for $Ca(Fe_{1/2}Ta_{1/2})O_3$ dense ceramics at different frequencies.

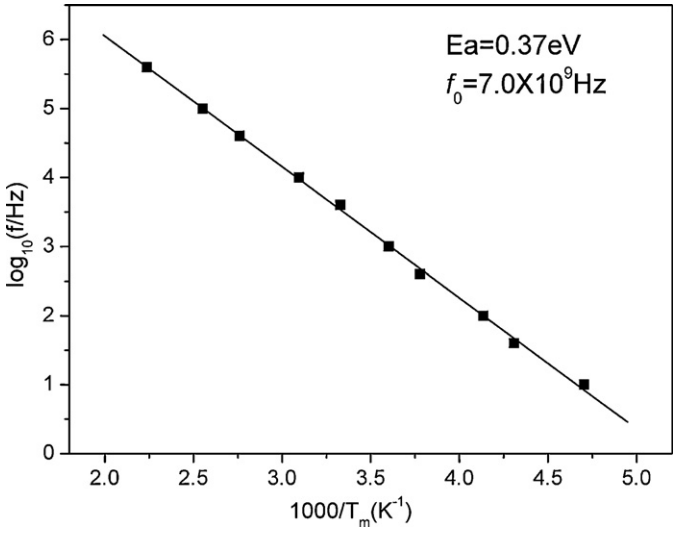

Fig. 5. Frequency dependence of the peak temperature of dielectric loss for low temperature dielectric relaxation in as-sintered $Ca(Fe_{1/2}Ta_{1/2})O_3$ ceramics. The experimental data have been fitted by Arrhenius law.

E_a = 0.37 eV and $f_0 = 7.0 \times 10^9$ Hz. As reported previously [8], the activation energy in $Sr(Fe_{1/2}Nb_{1/2})O_3$ ceramic is 0.38 eV. The close activation energy E_a for the present material and $Sr(Fe_{1/2}Nb_{1/2})O_3$ indicates that the physical origin of the low

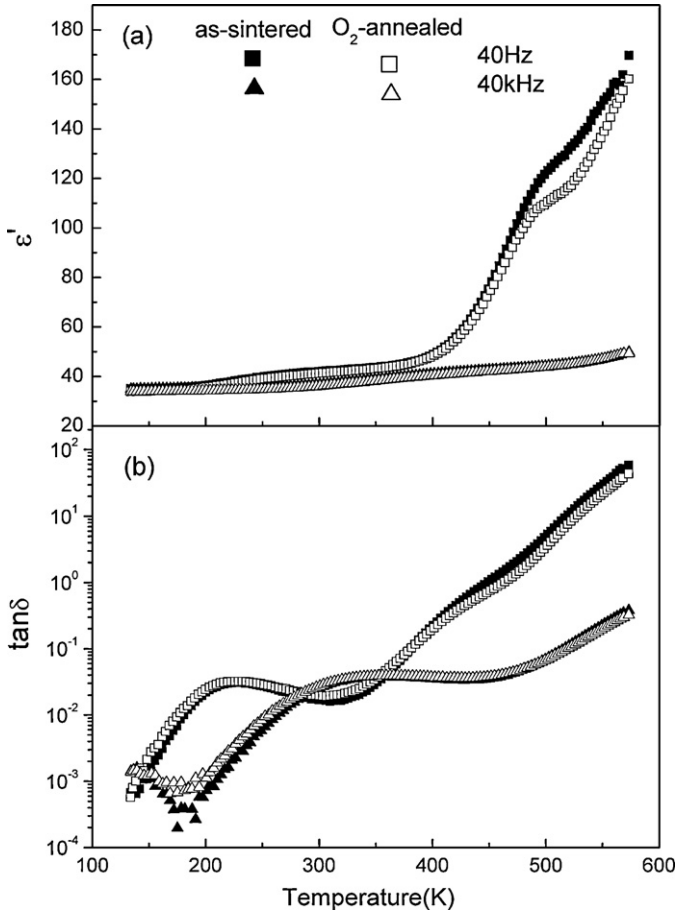

Fig. 6. Effects of oxygen annealing upon (a) dielectric constant and (b) dielectric loss of $Ca(Fe_{1/2}Ta_{1/2})O_3$ dense ceramics.

temperature dielectric relaxation in $Ca(Fe_{1/2}Ta_{1/2})O_3$ should be similar to that in $Sr(Fe_{1/2}Nb_{1/2})O_3$.

As shown in Fig. 6, the effects of oxygen annealing upon dielectric constant and dielectric loss $Ca(Fe_{1/2}Ta_{1/2})O_3$ ceramics are very weak compared with $R(Fe_{1/2}M_{1/2})O_3$ (R = Ba, Sr; M = Ta, Nb). The low temperature dielectric relaxation is almost not affected by O_2 annealing. The shoulder-like high temperature dielectric anomality is little smaller than the as-sintered ceramics, and only a very slight decrease is detected in dielectric loss. To figure out the physical origin of the two dielectric relaxations, the mixed-valent structures in as-sintered $Ca(Fe_{1/2}Ta_{1/2})O_3$ and O_2-annealed $Ca(Fe_{1/2}Ta_{1/2})O_3$ ceramics were investigated by XPS.

Fig. 7 shows the XPS spectra of Fe 2p of as-sintered $Ca(Fe_{1/2}Ta_{1/2})O_3$ ceramics and annealed $Ca(Fe_{1/2}Ta_{1/2})O_3$ ceramics. The $2p_{3/2}$ peak for Fe can be split into two peaks by a Gaussian–Lorentzian curve fitting, which shows the existence of Fe^{2+} in addition to Fe^{3+} ions. The binding energy for Fe^{2+} $2p_{3/2}$ and Fe^{3+} $2p_{3/2}$ is 710.5 eV and 711.6 eV, respectively. By fitting the peaks, the oxidation states of Fe^{3+} and Fe^{2+} in as-sintered and annealed ceramics are 16:5 and 17:5 ($\Sigma\chi^2$ are smaller than 1) by XPSPEAK Version 4.0, respectively. The results of the XPS measurement indicate that the O_2-annealing have little effect in reducing the O_2 vacancies in $Ca(Fe_{1/2}Ta_{1/2})O_3$ ceramics, which is in good agreement with the effects of oxygen annealing upon

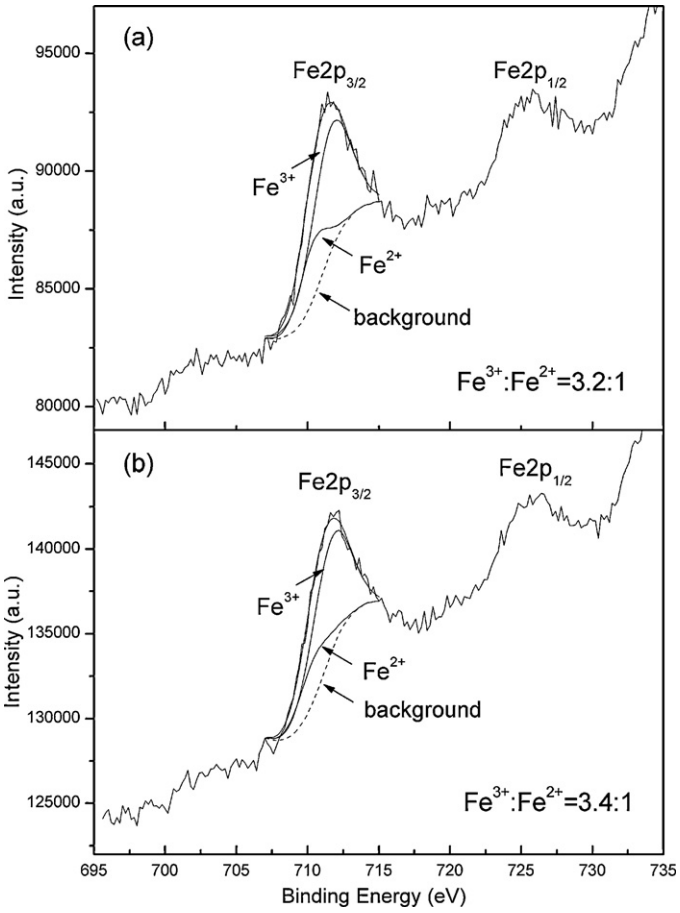

Fig. 7. XPS spectra of $Fe2p_{3/2}$ for $Ca(Fe_{1/2}Ta_{1/2})O_3$ dense ceramics: (a) as-sintered and (b) annealed in oxygen for 6 h.

Table 3
Microwave dielectric characteristics of $Ca(Fe_{1/2}Ta_{1/2})O_3$ dense ceramics.

Samples	f_0 (GHz)	ε_r	Qf (GHz)
As-sintered	5.38	30.7	3070
Annealed	5.38	30.6	3450

dielectric constant and dielectric loss of $Ca(Fe_{1/2}Ta_{1/2})O_3$ dense ceramics in Fig. 6. Furthermore, the oxygen vacancy in $Ca(Fe_{1/2}Ta_{1/2})O_3$ ceramics is much less than that in $Ba(Fe_{1/2}Nb_{1/2})O_3$ ceramics [18].

The microwave dielectric properties of $Ca(Fe_{1/2}Ta_{1/2})O_3$ ceramics are listed in Table 3 The as-sintered and O_2-annealed $Ca(Fe_{1/2}Ta_{1/2})O_3$ ceramics have almost the same f_0 (5.38 GHz) and dielectric constant (~30.6), while the O_2-annealing slightly improved the Qf of $Ca(Fe_{1/2}Ta_{1/2})O_3$ ceramics. The Qf for O_2-annealed $Ca(Fe_{1/2}Ta_{1/2})O_3$ ceramics is 3450 GHz, which is slightly higher than that in the as-sintered $Ca(Fe_{1/2}Ta_{1/2})O_3$ ceramics (3070 GHz). The results are also in good agreement with the XPS results.

4. Conclusions

The complex perovskite $Ca(Fe_{1/2}Ta_{1/2})O_3$ dense ceramics can be obtained by sintering at 1523 K in air for 3 h. Two dielectric relaxations are observed in the low and high temperature ranges, respectively. Compared with $Ba(Fe_{1/2}Ta_{1/2})O_3$, $Sr(Fe_{1/2}Ta_{1/2})O_3$ and $Ba(Fe_{1/2}Nb_{1/2})O_3$, the much lower dielectric constant and lower dielectric loss are determined in $Ca(Fe_{1/2}Ta_{1/2})O_3$ because of the obviously weaker Fe^{2+}/Fe^{3+} mixed-valent structure. The microwave dielectric properties (at 5.38 GHz) for $Ca(Fe_{1/2}Ta_{1/2})O_3$ ceramics are obtained as: $\varepsilon_r = 30.7$, $Qf = 3.07$ GHz.

Acknowledgments

The present work was financially supported by Natural Science Foundation of China under grant number 50832005 and National Basic Research Program of China under grant number 2009CB929503.

References

[1] D. Viehlan, J.F. Li, S.J. Jang, L.E. Cross, M. Wutting, Dipolar-glass model for lead magnesium niobate, Phys. Rev. B 43 (10) (1991) 8316.
[2] K. Kakegawa, J. Mohri, T. Takahashi, H. Yamamura, S. Shirasaki, A compositional fluctuation and properties of Pb(Zr, Ti)O_3, Solid State Commun. 24 (11) (1977) 769–772.
[3] G.A. Smolenskii, A.I. Agranovuskaya, Dielectric polarization of a number of complex compounds, Sov. Phys. Solid State 1 (1959) 1429–1437.
[4] D.S. Fu, H. Taniguchi, M. Itoh, S. Koshihara, N. Yamamoto, S. Mori, Relaxor ''Pb(Mg1/3Nb2/3)O3: a ferroelectric with multiple inhomogeneities'', Phys. Rev. Lett. 103 (20) (2009) 207601.
[5] T.A. Vanderah, Talking ceramics, Science 298 (2002) 1182–1184.
[6] R.J. Cava, Dielectric materials for applications in microwave communications, J. Mater. Chem. 11 (2001) 54–62.
[7] S. Kawashima, M. Nishida, I. Ueda, H. Ouchi, $Ba(Zn_{1/3}Ta_{2/3})O_3$ ceramics with low dielectric loss at microwave frequencies, J. Am. Ceram. Soc. 66 (6) (1983) 421–423.
[8] Z. Wang, X.M. Chen, L. Ni, X.Q. Liu, Dielectric abnormities of complex perovskite $Ba(Fe_{1/2}Nb_{1/2})O_3$ ceramics over broad temperature and frequency range, Appl. Phys. Lett. 90 (2) (2007) 022904.
[9] Z. Wang, X.M. Chen, L. Ni, Y.Y. Liu, X.Q. Liu, Dielectric relaxations in $Ba(Fe_{1/2}Ta_{1/2})O_3$ giant dielectric constant ceramics, Appl. Phys. Lett. 90 (10) (2007) 102905.
[10] Y.Y. Liu, X.M. Chen, X.Q. Liu, L. Li, Giant dielectric response and relaxor behaviors induced by charge and defect ordering in Sr(Fe1/2Nb1/2)O3 ceramics, Appl. Phys. Lett. 90 (19) (2007) 102905.
[11] Y. Liu, X.M. Chen, X.Q. Liu, L. Li, Dielectric relaxations in $Ca(Fe_{1/2}Nb_{1/2})O_3$ complex perovskite ceramics, Appl. Phys. Lett. 90 (26) (2007) 262904.
[12] J.R. Carvajal, Recent Developments of the Program FULLPROF, in the Commission on the Powder Diffraction (IUCr), Int. Union Crystallogr. Newsl. 26 (2001) 12–19.
[13] D. Kajfez, P. Guillon, Dielectric Resonators, 2nd edition, Noble Publishing Corporation, Atlanta, 1998.
[14] L. Farber, M. Valant, M.A. Akbas, P.K. Davies, Cation ordering in $Pb(Mg_{1/3}Nb_{2/3})O_3$–$Pb(Sc_{1/2}Nb_{1/2})O_3$ (PMN–PSN) solid solutions, J. Am. Ceram. Soc. 85 (2002) 2319–2324.
[15] I.M. Reaney, E.L. Collar, N. Setter, Dielectric and structure characteristics of Ba- and Sr-based complex perovskites as a function of tolerance factor, Jpn. J. Appl. Phys. 33 (7A) (1994) 3984–3990.
[16] A.M. Glazer, Simple ways of determining perovskite structures, Acta Cryst. A31 (1975) 756–762.
[17] A.M. Glazer, The classification of tilted octahera in perovskites, Acta Cryst. B28 (1972) 2284–2292.
[18] Z. Wang, X.M. Chen, X.Q. Liu, $Ba[(Fe_{0.9}Al_{0.1})_{0.5}Ta_{0.5}]O_3$ ceramics with extended giant dielectric constant step and reduced dielectric loss, J. Appl. Phys. 105 (2009) 034114.
[19] F. Izumi, R.A. Dilanian, Recent Research Development in Physics, vol. 3, Part II, Transworld Research Network, Trivandrum, 2002, pp. 699–726, ISBN 81-7895-046-4.